Journal of the Ceramic Society of Japan 133 [6] 242-245 2025
DOI https://doi.org/10.2109/jcersj2.25042

JCS-Japan

EXPRESS LETTER

Formation of triclusters in silica melt under high pressure

Shino Hayafune[1,2], Tatsuya Sakamaki[1], Haruki Ichikawa[1], Yohei Onodera[2], Shinji Kohara[2,†] and Akio Suzuki[1]

[1] Department of Earth Science, Graduate School of Science, Tohoku University, Sendai 980–8578, Japan
[2] Center for Basic Research on Materials, National Institute for Materials Science, Ibaraki 305–0047, Japan

Silica (SiO_2) is the major glass-forming material, and the structures of silica glass and melt have been extensively studied using X-ray and neutron diffraction techniques. The diffraction data of silica glass and melt show the first sharp diffraction peak (FSDP) at $Q \sim 1.5$ Å^{-1}, which is a signature of intermediate-range order. In this study, we performed classical molecular dynamics (MD) simulations at 2000 K and 5 GPa to understand the behaviour of the diffraction peak associated with the modification of intermediate-range order. The high-pressure melt data obtained show the decrease in the height of FSDP with a shift of the peak position to the high-Q side in X-ray diffraction data, although the average coordination number of four was maintained. In addition, we observed the formation of OSi_3 triclusters, which share an oxygen atom with a SiO_4 tetrahedron. This unusually dense packed atomic arrangement is the result of high pressure and is associated with the very sharp principal peak observed at $Q \sim 3$ Å^{-1} in the O–O partial structure factor derived by MD simulation.

Key-words : Silica, High pressure melt, Molecular dynamics simulation

[Received March 17, 2025; Accepted April 9, 2025; Published online April 25, 2025]

Glass is abundant in nature and has been manufactured by humans for more than 3000 years. Glass has evolved from basic structural materials such as art objects and window glasses to advanced electronic products, biological products, photon products, and functional materials such as mass-produced window and fibre glasses. Silica is the main oxide material for window, optical, and fibre glasses. The atomic structure of silica glass has been extensively studied using quantum beam (X-ray and neutron) diffraction techniques because the diffraction data are very sensitive to the intermediate-range order.[1–10] Silica glass and melt exhibit a first sharp diffraction peak (FSDP)[1–5,11,12] at $Q \sim 1.5$ Å^{-1} in both X-ray and neutron diffraction data. The FSDP is a signature of intermediate-range order manifested by a periodicity of 4 Å and a coherence length of 10 Å.[5] The peak position and height are significantly affected by temperature and pressure. Many diffraction studies of silica glass under the conditions ranging from ambient temperature/pressure to high pressure,[11–22] have been reported, but we are not aware of diffraction data of silica melt under high pressure/temperature due to experimental difficulties. The structural changes of silica melt under compression have been revealed by classical or first-principles molecular dynamics (MD) simulations.[23–25]

In this article, we report the results of classical MD simulation of silica melt to understand the behaviour of diffraction peaks associated with the modification of intermediate-range order under high pressure in comparison with previously reported X-ray diffraction[12] and MD simulation[26] data of silica melt at ambient pressure and hot-compressed silica glasses.[22]

MD simulations of the SiO_2 melt were performed using the Large-scale Atomic/Molecular Massively Parallel Simulator code.[27] The number of particles was 30000. We employed the empirical force field developed by Guillot and Sator[28] with the NPT ensemble. The pressure was kept at 5 GPa and the temperature at 2000 K. The atomic number density was 0.08635 Å^{-3}. Ewald summations were used to evaluate long-range Coulombic interactions. Periodic boundary conditions were imposed in the simulations, and the time step was 1 fs. The simulations were started with random configuration and velocity. We first ran calculations for 50 ps at 5 GPa and 3000 K. The system was then cooled to 2000 K for 10 ps and relaxed for 50 ps.

Figure 1 shows the X-ray structure factor $S(Q)$ of silica glass at ambient pressure together with the X-ray $S(Q)$ of silica melt at ambient pressure and 5 Gpa. Experimental data of both silica glass (blue)[29] and melt (cyan)[12] under ambient conditions show prominent FSDPs at $Q \sim 1.5$ Å^{-1}, although the peak height of the melt is smaller than that of the glass owing to the high temperature. The MD data reported by Takada et al. (red)[26] is in very good agreement with the experimental data (cyan) reported by Skinner et al.[12] Our simulation data (black) for the high-pressure melt shows an FSDP at $Q \sim 1.9$ Å^{-1}, which is a higher Q value owing to the high pressure (27 % densification), but the peak height of the high-pressure melt is identical to that of the ambient-pressure melt.

† Corresponding author: S. Kohara; E-mail: KOHARA.Shinji@nims.go.jp

Figure 2(a) shows the partial pair distribution functions $g_{ij}(r)$ of silica melts obtained by MD simulation. Both the ambient- and high-pressure melts show a prominent Si–O correlation peak at 1.6 Å, but the peak width decreases in the high-pressure melt owing to the high pressure. Indeed, the average Si–O coordination number for both melts is approximately four. The Si–O correlation of the ambient-pressure melt shows a zero-correlation region at 2.2–2.8 Å, but this region almost disappears in the high-pressure melt. The O–O $g_{ij}(r)$ of the two melts are identical because the intratetraheral O–O correlation is dominant in real space, whereas the Si–Si $g_{ij}(r)$ of the two melts are significantly different because the Si–Si correlation describes the correlation of the centres of SiO_4 tetrahedra, which is significantly modified because of cavity squeezing[22] by densification.

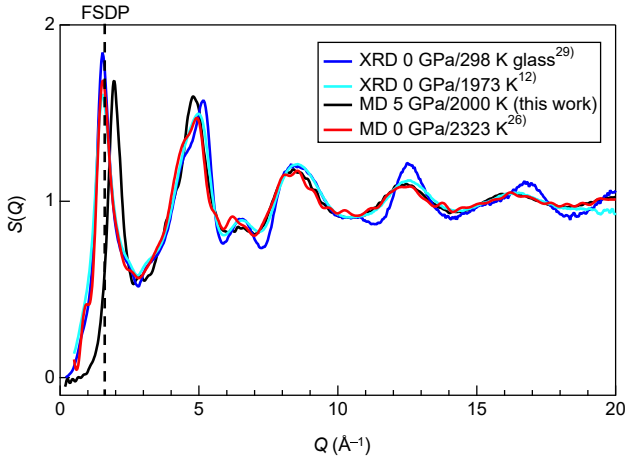

Fig. 1. X-ray structure factor $S(Q)$ of silica glass at ambient pressure together with X-ray $S(Q)$ of silica melt at ambient pressure and 5 GPa.

Figure 2(b) shows the partial structure factors $S_{ij}(Q)$ of silica melts obtained by MD simulation. The three $S_{ij}(Q)$ have a positive peak at the FSDP position, which is in line with the behaviour of the glass under ambient conditions.[5,22] They show the peak shifting to the high-Q side under high pressure similarly to the FSDP of X-ray $S(Q)$ shown in Fig. 1, but show a sharp constant in the high-pressure melt: both the heights of the Si–O and O–O FSDPs decrease, whereas that of the Si–Si FSDP increases. This behaviour is identical to that of hot compressed glass as reported by Onodera et al.[22] In addition, a positive principal peak (PP)[2] is found for Si–Si and O–O $S_{ij}(Q)$, while a negative PP is found for Si–O $S_{ij}(Q)$ at $Q \sim 3$ Å^{-1}. According to Zeidler and Salmon, the PP observed in neutron diffraction data reflects the packing fraction of the oxygen atoms because neutrons are sensitive to the O–O correlation.[30,31] This behaviour suggests that a large difference in the height of the PP in O–O $S_{ij}(Q)$ reflects the difference in the packing fraction of the oxygen atoms associated with cavity squeezing[22] by densification. We also suggest that the negative PP in Si–O $S_{ij}(Q)$ reflects the zero-correlation region in Si–O $g_{ij}(r)$ in Fig. 2(a) caused by the chemical difference between silicon (fourfold) and oxygen (twofold) atoms.

Figure 3 shows the bond angle distributions (BADs) of the silica melts obtained by MD simulation. O–Si–O BAD shows the symmetry of SiO_4 tetrahedra, suggesting that this symmetry is maintained in the high-pressure melt. A peak observed at 60° of O–O–O BAD reflects O–O–O triangles in a SiO_4 tetrahedron and intertetrahedral O–O–O correlation.[32] The difference between ambient- and high-pressure melts is small. The profiles observed at angles greater than 80° reflect intertetrahedral O–O–O correlation, in which a significant difference is observed. Si–Si–Si BAD reflects

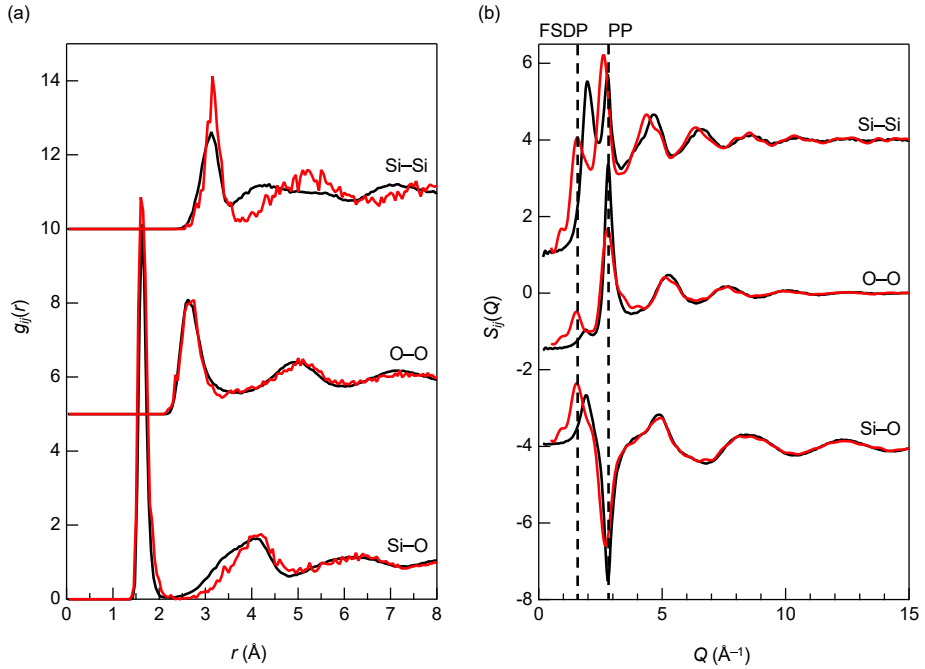

Fig. 2. Partial pair distribution functions $g_{ij}(r)$ (a) and partial structure factors $S_{ij}(Q)$ (b) of silica melts obtained by MD simulation. Black curves, 5 GPa/2000 K; red curves, 0 GPa/2323 K.[26]

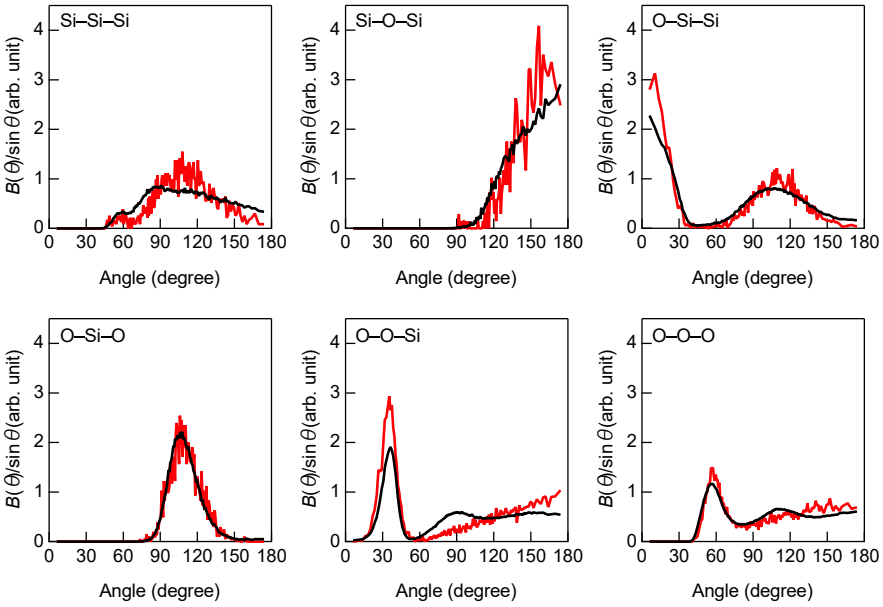

Fig. 3. Bond angle distributions of the silica melts obtained by MD simulation. Black curves, 5 GPa/2000 K; red curves, 0 GPa/2323 K.[26)]

the symmetry of intertetrahedral Si–(O)–Si_4 hypertetrahedra.[21,22,30)] The symmetry of hypertetraheda of ambient-pressure melt is far from that of the regular tetrahedra of silica glass,[22,32)] and the symmetry is broken in the high-pressure melt similarly to the glass under high pressure as reported by Kono et al.[21)] Si–O–Si BAD reflects the intertetrahedral correlation and has been extensively discussed.[33)] The ambient-pressure melt has a peak at ~150°, whereas the high-pressure melt does not have a well-defined peak. This behaviour is similar to the difference between pristine and hot-compressed glasses,[22)] and far from the recent results obtained by machine learning MD simulation, which shows a large difference in peak position between pristine and hot-compressed glasses.[34)] O–Si–Si BAD also reflects intertetrahedral correlation, and the peak heights observed at ~15° and ~105° decrease in the high-pressure melt, which is consistent with the behaviour of the hot-compressed glass.[22)] O–O–Si BAD reflects both intra- and intertetrahedral correlations, which shows significant differences between ambient- and high-pressure melts. The peak profile of the ambient-pressure melt is identical to that of the hot-compressed glass reported by Onodera et al.,[22)] but that of the high-pressure melt is very different from that of the hot-compressed glass. The peak observed at ~30° indicates the intratetrahedral O–O–Si correlation, the peak height of which is smaller in the high-pressure melt than that in the ambient-pressure melt. However, the peak profile in the large-angle (>60°) region of the high-pressure melt, which is considered to indicate the intertetrahedral O–O–Si correlation, is far from that of the ambient-pressure melt. This behaviour is similar to that of O–O–O BAD, and understanding O–O–Si and O–O–O BADs is important to understand the structure of the high-pressure melt.

On the basis of the above discussion, we attempted to analyse the intertetrahedral correlation. We calculated the

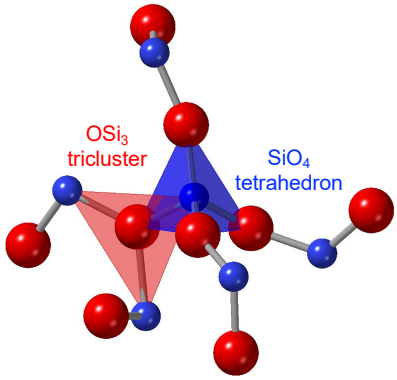

Fig. 4. Typical atomic arrangement formed by the combination of a SiO_4 tetrahedron and an OSi_3 tricluster. Only the highlighted oxygen atom forms a tricluster.

fraction of OSi_3 triclusters in the melts and found that it is only 0.3 % in the ambient-pressure melt, but it is approximately ten times higher in the high-pressure melt. The typical local atomic arrangement of an OSi_3 tricluster combined with a SiO_4 tetrahedron is illustrated in **Fig. 4**. Note that the number of silicon atoms around the silicon atom in the centre of the SiO_4 tetrahedron is five, although the number of bridging oxygen atoms around the silicon atom in the centre of SiO_4 tetrahedron is four. The formation of the tricluster is out of Zachariasen's rule,[35)] where oxygen atoms should be twofold, and we suggest that this unusual atomic arrangement in silica melt is induced by high pressure. It is also shown that this highly densely packed atomic arrangement is associated with the very sharp PP in the O–O $S_{ij}(Q)$ observed at $Q \sim 3$ Å^{-1} in Fig. 2(b). In addition, this atomic arrangement is consistent with the "zip model" proposed by Zeidler et al.[18)] for silica glass under high pressure at room temperature.

In this article, we have presented the results of classical MD simulation of the silica melt under high pressure.

The comparison with the ambient-pressure melt and hot-compressed glass is very useful for understanding the effect of pressure on the intermediate-range order of the melt manifested by FSDP and PP in diffraction data. We found a very unusually densely packed atomic arrangement in the high-pressure melt, and it is likely that such an arrangement is also observed in amorphous alumina (Al_2O_3) because it has a large number of triclusters.[36] We also suggest that this atomic arrangement indicates the onset of the transformation from four- to five- and sixfold Si–O polyhedra through the recombination of Si–O bonds.

Acknowledgments We are grateful to Dr. Akira Takada for providing the MD simulation data of silica melt at ambient pressure. This research was carried out with the support of JSPS KAKENHI Grant Numbers 20H05878, 20H05881, JP21K18641, and JP23K22588. MD simulations were performed using the Numerical Materials Simulator at the National Institute for Materials Science (NIMS).

References

1) D. L. Price, S. C. Moss, R. Reijers, M.-L. Saboungi and S. Susman, *J. Phys. C Solid State* **21**, L1069 (1988).
2) P. S. Salmon, R. A. Martin, P. E. Mason and G. J. Cuello, *Nature* **435**, 75 (2005).
3) G. N. Greaves and S. Sen, *Adv. Phys.* **56**, 1 (2007).
4) S. R. Elliott, *Nature* **354**, 445 (1991).
5) Y. Onodera, S. Kohara, S. Tahara, A. Masuno, H. Inoue, M. Shiga, A. Hirata, K. Tsuchiya, Y. Hiraoka, I. Obayashi, K. Ohara, A. Mizuno and O. Sakata, *J. Ceram. Soc. Jpn.* **127**, 853 (2019).
6) K. A. Kirchner, D. R. Cassar, E. D. Zanotto, M. Ono, S. H. Kim, K. Doss, M. L. Bødker, M. M. Smedskjaer, S. Kohara, L. Tang, M. Bauchy, C. J. Wilkinson, Y. Yang, R. S. Welch, M. Mancini and J. C. Mauro, *Chem. Rev.* **123**, 1774 (2023).
7) S. Kohara and P. S. Salmon, *Adv. Phys.: X* **1**, 640 (2016).
8) S. Kohara, *J. Ceram. Soc. Jpn.* **125**, 799 (2017).
9) S. Kohara, *J. Ceram. Soc. Jpn.* **130**, 531 (2022).
10) Y. Onodera, *J. Ceram. Soc. Jpn.* **130**, 627 (2022).
11) Q. Mei, C. J. Benmore and J. K. R. Weber, *Phys. Rev. Lett.* **98**, 057802 (2007).
12) L. B. Skinner, C. J. Benmore, J. K. R. Weber, M. C. Wilding, S. K. Tumber and J. B. Parise, *Phys. Chem. Chem. Phys.* **15**, 8566 (2013).
13) C. Meade, R. J. Hemley and H. K. Mao, *Phys. Rev. Lett.* **69**, 1387 (1992).
14) Y. Inamura, Y. Katayama, W. Utsumi and K. Funakoshi, *Phys. Rev. Lett.* **93**, 015501 (2004).
15) T. Sato and N. Funamori, *Phys. Rev. Lett.* **101**, 255502 (2008).
16) C. J. Benmore, E. Soignard, S. A. Amin, M. Guthrie, S. D. Shastri, P. L. Lee and J. L. Yarger, *Phys. Rev. B* **81**, 054105 (2010).
17) T. Sato and N. Funamori, *Phys. Rev. B* **82**, 184102 (2010).
18) A. Zeidler, K. Wezka, R. F. Rowlands, D. A. J. Whittaker, P. S. Salmon, A. Polidori, J. W. E. Drewitt, S. Klotz, H. E. Fischer, M. C. Wilding, C. L. Bull, M. G. Tucker and M. Wilson, *Phys. Rev. Lett.* **113**, 135501 (2014).
19) M. Murakami, S. Kohara, N. Kitamura, J. Akola, H. Inoue, A. Hirata, Y. Hiraoka, Y. Onodera, I. Obayashi, J. Kalikka, N. Hirao, T. Musso, A. S. Foster, Y. Idemoto, O. Sakata and Y. Ohishi, *Phys. Rev. B* **99**, 045153 (2019).
20) Y. Kono, Y. Shu, C. Kenney-Benson, Y. Wang and G. Shen, *Phys. Rev. Lett.* **125**, 205701 (2020).
21) Y. Kono, K. Ohara, N. M. Kondo, H. Yamada, S. Hiroi, F. Noritake, K. Nitta, O. Sekizawa, Y. Higo, Y. Tange, H. Yumoto, T. Koyama, H. Yamazaki, Y. Senba, H. Ohashi, S. Goto, I. Inoue, Y. Hayashi, K. Tamasaku, T. Osaka, J. Yamada and M. Yabashi, *Nat. Commun.* **13**, 2292 (2022).
22) Y. Onodera, S. Kohara, P. S. Salmon, A. Hirata, N. Nishiyama, S. Kitani, A. Zeidler, M. Shiga, A. Masuno, H. Inoue, S. Tahara, A. Polidori, H. E. Fischer, T. Mori, S. Kojima, H. Kawaji, A. I. Kolesnikov, M. B. Stone, M. G. Tucker, M. T. McDonnell, A. C. Hannon, Y. Hiraoka, I. Obayashi, T. Nakamura, J. Akola, Y. Fujii, K. Ohara, T. Taniguchi and O. Sakata, *NPG Asia Mater.* **12**, 85 (2020).
23) J. R. Rustad, D. A. Yuen and F. J. Spera, *Phys. Rev. A* **42**, 2081 (1990).
24) B. B. Karki, D. Bhattarai and L. Stixrude, *Phys. Rev. B* **76**, 104205 (2007).
25) V. H. Nguyen and H. A. Nguyen, *Pramana-J. Phys.* **98**, 142 (2024).
26) A. Takada, P. Richet, C. R. A. Catlow and G. D. Price, *J. Non-Cryst. Solids* **345–346**, 224 (2004).
27) A. P. Thompson, H. M. Aktulga, R. Berger, D. S. Bolintineanu, W. M. Brown, P. S. Crozier, P. J. In 'T Veld, A. Kohlmeyer, S. G. Moore, T. D. Nguyen, R. Shan, M. J. Stevens, J. Tranchida, C. Trott and S. J. Plimpton, *Comput. Phys. Commun.* **271**, 108171 (2022).
28) B. Guillot and N. Sator, *Geochim. Cosmochim. Ac.* **71**, 4538 (2007).
29) S. Sato, M. Miyakawa, T. Taniguchi, Y. Onodera, K. Ohara, K. Ikeda, N. Kitamura, Y. Idemoto and S. Kohara, *J. Ceram. Soc. Jpn.* **132**, 427 (2024).
30) P. S. Salmon and A. Zeidler, *J. Stat. Mech.-Theory E* **2019**, 114006 (2019).
31) A. Zeidler, P. S. Salmon and K. B. Skinner, *P. Natl. Acad. Sci. USA* **111**, 10045 (2014).
32) S. Kohara, S. Sato, M. Shiga, Y. Onodera, H. Masai, T. Wakihara, A. Masuno, A. Hirata, N. Kitamura, Y. Idemoto, K. Kimura and K. Hayashi, *J. Ceram. Soc. Jpn.* **132**, 653 (2024).
33) M. G. Tucker, D. A. Keen, M. T. Dove and K. Trachenko, *J. Phys. Condens. Matter* **17**, S67 (2005).
34) K. Kobayashi, M. Okumura, H. Nakamura, M. Itakura, M. Machida, S. Urata and K. Suzuya, *Sci. Rep.-UK* **13**, 18721 (2023).
35) W. H. Zachariasen, *J. Am. Chem. Soc.* **54**, 3841 (1932).
36) H. Hashimoto, Y. Onodera, S. Tahara, S. Kohara, K. Yazawa, H. Segawa, M. Murakami and K. Ohara, *Sci. Rep.-UK* **12**, 516 (2022).